Surprising importance of photo-assisted etching of silicon in chlorine-containing plasmas

Hyungjoo Shin, Weiye Zhu, Vincent M. Donnelly,[a] and Demetre J. Economou[b]
Plasma Processing Laboratory, Department of Chemical and Biomolecular Engineering, University of Houston, 4800 Calhoun Road, Houston, Texas 77204

(Received 29 November 2011; accepted 11 January 2012; published 6 February 2012)

The authors report a new, important phenomenon: photo-assisted etching of *p*-type Si in chlorine-containing plasmas. This mechanism was discovered in mostly Ar plasmas with a few percent added Cl_2, but was found to be even more important in pure Cl_2 plasmas. Nearly monoenergetic ion energy distributions (IEDs) were obtained by applying a synchronous dc bias on a "boundary electrode" during the afterglow of a pulsed, inductively coupled, Faraday-shielded plasma. Such precisely controlled IEDs allowed the study of silicon etching as a function of ion energy, at near-threshold energies. Etching rates increased with the square root of the ion energy above the observed threshold of 16 eV, in agreement with published data. Surprisingly, a substantial etching rate was observed, independent of ion energy, when the ion energy was below the ion-assisted etching threshold. Experiments ruled out chemical etching by Cl atoms, etching assisted by Ar metastables, and etching mediated by holes and/or low energy electrons generated by Auger neutralization of low-energy ions, leaving photo-assisted etching as the only likely explanation. Experiments were carried out with light and ions from the plasma either reaching the surface or being blocked, showing conclusively that the "sub-threshold" etching was due to photons, predominately at wavelengths < 1700 Å. The photo-assisted etching rate was equal to the ion-assisted etching rate at 36 eV, causing substantial complications for processes that require low ion energies to achieve high selectivity and low damage, such as atomic layer etching. Under these conditions, photo-assisted etching likely plays an important role in profile evolution of features etched in Si with chlorine-containing plasmas, contributing to the commonly observed sloped sidewalls and microtrenches. © *2012 American Vacuum Society*. [DOI: 10.1116/1.3681285]

I. INTRODUCTION

In 1979 Coburn and Winters published a classic paper that for the first time put forth strong evidence for the mechanism for anisotropic etching of silicon in a plasma.[1] In that study, they found a synergistic effect between positive ion (Ar^+) bombardment and neutral (XeF_2 or Cl_2) impingement. Before this, it was not known whether ions, electrons, or even photons were the important energetic species. In fact, Coburn and Winters also investigated the role of electrons and found them to be much less important. The role of photons was not considered in these studies. Indeed, at the high ion energies used in that study (450 eV), positive ions played the dominant role by far in inducing etching.

More recently, however, there has been increasing interest in operating at much lower ion energies (10 s of eV) to improve selectivity and reduce damage. When operating near the threshold for ion-assisted etching, it is possible to achieve selectivities of Si etching with respect to SiO_2 of greater than 100:1.[2] As device feature sizes shrink below 22 nm, precise etching with less damage using low energy ions is necessary. With such low ion energies, the etching rate is greatly reduced, making it possible for the contribution of p'hoto-assisted etching to become significant.

Photon-induced etching of Si with halogen in the absence of a plasma has been studied by several researchers. Using ultraviolet (UV) light from a Hg–Xe lamp, Okano *et al.*[3] showed that undoped poly-Si cannot be etched with Cl atoms alone, generated by photodissociation of Cl_2 gas. When the light was directed at the sample, however, slow etching of Si (4 nm/min) was observed. They attributed the etching to a field-assisted diffusion of Cl^- into the Si lattice as in oxidation, originally proposed by Mott and Cabrera.[4,5] Houle[6] used an Ar^+ ion laser (514.5 nm, up to 6 W, unfocussed) to study the photochemical etching of Si by XeF_2. She showed that photo-generated charge carriers enhance etching by causing desorption of SiF_3, and found no evidence of field-assisted diffusion. Photo-generated carriers have also been shown to induce etching of *p*-type Si in Cl_2 under the irradiation of a pulsed 308 nm XeCl excimer laser,[7] or a continuous wave Ar^+ or Kr^+ laser at various wavelengths.[8] Similar to the mechanism reported by Houle, Jackman *et al.*[9] have shown that UV irradiation of Si in Cl_2 causes a conversion of strongly adsorbed species into more weakly bound groups, leading to enhanced desorption and etching. More recently, Samukawa *et al.*[10] showed that 220–380 nm radiation increases the etching rate of Si in a Cl atom beam at UV lamp power densities >20 mW/cm^2. They attributed the increased etching to crystal defects, created by the UV light, that are more susceptible to reaction with etchants.

The above studies were performed in a nonplasma environment, usually at much higher photon fluxes than those

[a]Electronic mail: vmdonnelly@uh.edu
[b]Electronic mail: economou@uh.edu

expected in etching plasmas, where the vast majority of the input power is consumed in processes other than the generation of light. To the best of our knowledge, *in situ* photo-assisted etching, arising from the light generated within the plasma itself, has not been reported. One reason is that in conventional plasma etching with relatively high energy ions (100 s of eV), photo-assisted etching is expected to be slow relative to ion-assisted etching. It is also hard to quantify ion-assisted etching in a plasma because the ion energy distribution (IED) is usually broad and the ion flux is often not well known.

The interactions of plasma-generated vacuum ultraviolet (VUV) photons with polymers and low-k materials have been reported. Wertheimer *et al.*[12] discussed the role of VUV radiation in the industrial processing of polymers. Nest *et al.*[13] clearly demonstrated synergetic effects of VUV exposure, ion bombardment, and heating on 193 nm photoresist surface roughening in plasma processing. Paragon *et al.*[14] also showed VUV light to be the main contributor to line-width roughness of 193 nm photoresist patterns in plasma etching. More recently, Lee and Graves[15] showed the effect of VUV photons from Ar and O_2 containing plasmas on chemical modification of porous SiOCH films.

In this study, etching by ions and photons was decoupled by controlling the energy of a narrow IED obtained by applying synchronous dc bias in the afterglow of a pulsed plasma.[11] With the well controlled IED and accurate ion current measurements, the etching yield for ion-assisted etching of Si in Cl_2/Ar plasmas was measured as a function of ion energy. While the threshold energy for ion-assisted etching and yields (Si per ion) compared well with published studies, a surprisingly large etching rate was found below the threshold for ion-assisted etching. This "sub-threshold" etching was independent of ion energy. Through a series of experiments with biased grids, optically opaque masks, and optically transmitting masks, it was determined conclusively that this sub-threshold etching is the result of illumination of the Si surface by light generated in the plasma, in particular, at VUV wavelengths.

II. EXPERIMENT

The plasma reactor depicted in Fig. 1 was equipped with periscopes for optical emission diagnostics, and an infrared (IR) laser interferometry setup. Details of the reactor, electronics for the pulsed plasma generation, and fundamental plasma characteristics are described in Ref. 11. The 13.56 MHz radio frequency (rf) inductively coupled plasma (ICP) was generated in a Faraday-shielded alumina tube. Either continuous or pulsed power was delivered through an L-matching network. The 5.08 cm diameter water-cooled stainless steel sample stage had a 2.64 cm diam. hole at the center, allowing either laser interferometry from the bottom side of the sample, as shown in Fig. 1, or the insertion of a 2.54 cm diameter stainless steel sample holder. Samples mounted on this holder could be transferred under vacuum to an ultrahigh vacuum chamber equipped with x-ray photoelectron spectroscopy. The sample holder temperature was

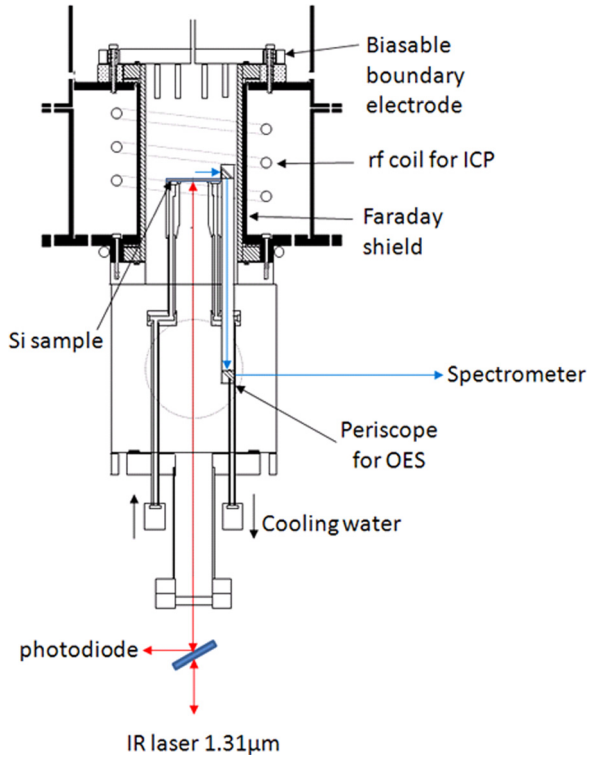

FIG. 1. (Color online) Schematic of the system used for experimental work. The Faraday-shielded inductively coupled plasma reactor was equipped with an IR laser interferometry setup for etching rate measurements, and optical emission diagnostics using a periscope to collect light near the sample surface. More details of the experimental apparatus can be found in Ref. 11.

controlled with a flow of water through a rod in contact with the bottom of the holder.

To maximize optical emission signals from Si etching products, a larger sample was used in many experiments. Si (100) p-type (B dopant density of 3×10^{14}–3×10^{15}/cm^3) wafers were cleaved into 5×5 cm^2 pieces and bonded to an electrically isolated, donut-shaped stainless steel disc on top of the grounded stage, using a silver-filled paste (Kurt J. Lesker Company, Pittsburgh, PA) for good thermal/electrical conduction. The Si sample covered the holder, minimizing sputtered contamination. The 500 μm thick substrates were polished on both sides, facilitating infrared (IR) laser interferometry measurements of etched thickness. The back side of the samples was scribed by a diamond tip to break native oxides and provide a good electrical contact. The current and hence ion flux to a sample was measured through an electrically isolated feedthrough.

Figure 2 shows a typical time-resolved current recorded by measuring the voltage drop across an 11.1 Ω resistor in series with the sample. During the active glow ($t = 0$–20 μs), the current fluctuated around zero, as expected. After the plasma is turned off, charge redistribution on the walls of the plasma reactor resulted in a slightly negative current flowing through the substrate. When a +20 V dc bias was applied on the boundary electrode (at $t = 70$ μs), the plasma potential was raised, blocking essentially all electron current to the substrate, to yield a positive current of ions bombarding the sample.

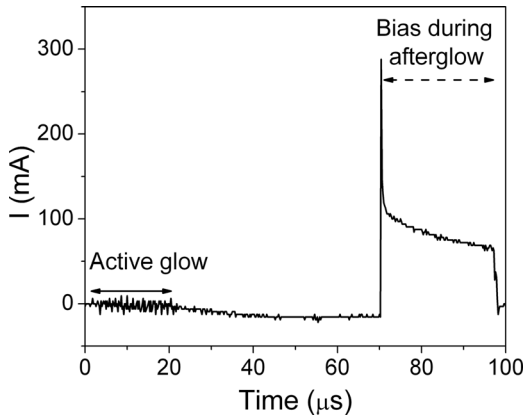

FIG. 2. Measured current to the substrate during the application of synchronous bias on the boundary electrode in the afterglow of a pulsed Ar ICP [10 kHz pulse frequency, 20 μs plasma ON (active glow), and 80 μs plasma OFF (afterglow)]. A +20 V dc bias was applied to the boundary electrode 50 μs into the afterglow (i.e., at $t = 70$ μs) until $t = 98$ μs.

In most experiments; however, a smaller sample and holder were transferred between a load-lock chamber and the plasma reactor, allowing many experiments to be performed without venting the plasma chamber. In addition, vacuum transfer of this sample holder to the XPS chamber allowed surface analysis on samples exposed to various plasma conditions and reactor materials. Despite a ten-fold reduction in sample size used for these experiments, ample Si emission signals were obtained, allowing the relative etching rate to be measured and converted into absolute values through calibrations, as described below. In addition, experiments to separately determine the role of positive ions, light, and light plus ions were carried out with this sample holder.

To either prevent or allow ions to bombard the surface, while also letting light and Cl atoms to impinge on the surface, a cage with two grids was fabricated and mounted on the sample stage [Fig. 3(a)]. Two tungsten mesh grids (each with 70% transmission and 180 μm square holes, Unique Wire Weaving Co., Hillside, NJ), were spot welded on a 1 mm thick stainless steel plate. The grids were separated by 2 mm and the sample was inserted in vacuum 2 mm below the bottom grid. After etching a Si sample in a Cl_2/Ar plasma, XPS showed only a small amount of tungsten chloride on the surface, if the substrate temperature were held at 80 °C, but much more if the sample were cooled to 20 °C. Consequently, measurements with the grids were carried out at 80 °C. [In experiments with the sample thermally floating, the Si emission intensity showed no obvious dependence on duration of plasma exposure, provided the native oxide was removed and the chamber walls were conditioned by etching Si for ~10 min prior. Laser interferometry measurements described below indicated that these initially room temperature, thermally floating samples reached temperatures of ~200 °C in a few minutes of etching at higher bias energies. Hence there appears to be little or no temperature dependence of the etching rate, and the measurements carried out with the grids at 80 °C can be compared with room temperature measurements without the grids. Also, these experiments were performed in a short time (a few minutes), using a fresh sample every time.]

The top grid could either be grounded or set to a small negative potential (V_A) to repel electrons and allow ions to enter. The bottom grid was initially intended to act as a switch, to turn ion bombardment ON or OFF by setting its potential (V_B) to either ground (ions ON) or sufficiently positive (ions OFF), with the ion energy being the difference between the substrate potential and the plasma potential. However, if substantial electron density was present between the grids, the positive potential on the bottom (repeller) grid could raise the plasma potential. If the plasma potential were to follow the repeller grid potential, the ions would always have higher energy than the repelling potential, leading to failure of ion filtering. To check this possibility, the potential on the floating boundary electrode (V_{BE}) was measured as positive potentials were applied to the repeller grid. The measured V_{BE} did indeed nearly track the repeller grid voltage (V_B), hence this configuration was abandoned. Instead, the potential of both grids (V_A and V_B) was set at −5 V (to repel low energy electrons and minimize heating of the grids) and the potential on the substrate (V_C) was used to both control ion energy and turn OFF all ion bombardment at sufficiently positive voltages. At the most positive voltage V_C required to reject all positive ions, V_{BE} barely increased (<1 V), indicating that there was no plasma potential perturbation.

The cage was not differentially pumped (to maintain, as much as possible, the plasma environment, such as the Cl

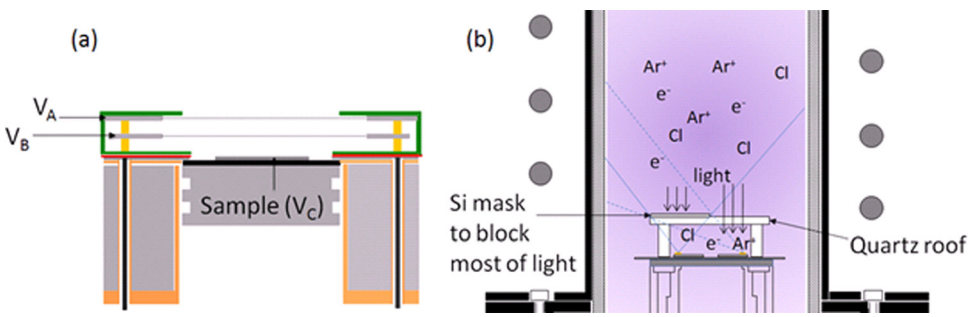

FIG. 3. (Color online) (a) Cage with two tungsten grids to test the role of low energy ions in sub-threshold etching. The sample was biased (V_C) to repel ions without disturbing the plasma potential. V_A and V_B were kept at −5 V. The distance from the top grid to the sample was 5 mm, and the distance between the two grids was 2 mm. (b) Schematic of a quartz roof placed 11 mm above the sample. Half of the roof was covered to make it opaque; the other half was transparent to light with wavelength above 170 nm.

atom density), and the distance from the top grid to the sample was 5 mm. For Ar^+ energies of a few tens of eV, the symmetric charge exchange cross section is 3×10^{-15} cm^2,[16–18] corresponding to mean free paths of 18 mm at 7 mTorr (the lowest pressure where the plasma can easily be sustained) and 2.5 mm at 50 mTorr and 80 °C. At 50 mTorr; therefore, the ions would suffer collisions (86% probability) while traversing the space between the top grid and the sample, creating energetic neutrals and lower energy ions. The lower energy ions would be repelled by the positive potential on the sample, but the energetic neutrals would strike the sample and corrupt the results. At 7 mTorr; on the other hand, the charge exchange probability is small (<25%) and the influence of fast neutrals is negligible (see Sec. III E).

Furthermore, the possible role of light, generated in the plasma, in inducing etching was investigated with a 20 mm by 40 mm quartz "roof" placed 11 mm above two samples, as shown in Fig. 3(b). Half of the roof was covered by a Si piece to block light and the other half transmitted light at wavelengths above 170 nm. Two Si samples were dipped into 48% HF solution, and one was placed beneath each region. The samples were therefore exposed to the same plasma and neutral density but very different levels of illumination from the relatively bright plasma closer to the center of the alumina tube. Each sample was covered with a small piece of Kapton tape on a symmetric location as a mask, and the etched depth was examined by a Tencor alpha step profilometer.

Two periscopes with UV transmitting prisms were attached to the sample holder. As shown in Fig. 1, light from the plasma near the substrate surface was directed to an optical emission spectrometer, consisting of a scanning monochromator and a GaAs photomultiplier tube (PMT). The monochromator had 1200 grooves/mm and, with a slit width of 100 μm, provided a resolution of 2.2 Å. The current from the PMT was amplified and collected by a data acquisition computer program. Optical emission from Si was used to obtain relative etching rates. The emission was time-averaged but was only excited during the plasma ON (active glow) fraction of the cycle.

As long as the plasma conditions remained constant and only the ion energy was varied to change the etching rate, the Si optical emission intensity should be proportional to the etching rate. To verify this and convert Si emission intensities into absolute etching rates, the etched depth was measured by infrared (IR) diode laser interferometry.[19–21] As shown in Fig. 1, the 1.31 μm laser was directed at the back of the sample. Reflected light from the top and the bottom surface of the double-side polished Si sample were recorded continuously and a number of interference fringes were observed. After the plasma was ignited, the optical path length within the sample increases due to heating and decreases as its thickness is reduced by etching. Initially, heating dominates, but as the temperature rise slows, the optical path length increases more slowly, stops (at fringe F_1), and then begins to decrease due to etching. After additional time, the plasma was extinguished and the number of fringes (F_2) was counted from when the optical path length first started to decrease until the sample cooled to a known final temperature (i.e., room temperature). The number of fringes caused only by etching was $\Delta N = F_2 - F_1$. The thickness change due to etching (Δd) was calculated from $\Delta d = \Delta N\, \lambda / 2n$, where $n = 3.5038$ is the index of refraction of Si at the laser wavelength, λ.[22]

As reported previously and reproduced in Fig. 4, the energy distribution of ions bombarding the substrate was controlled by changing pressure and by applying a synchronous direct current (dc) bias voltage to a boundary electrode during part of the afterglow.[11] The Faraday shield on the ICP reactor prevented capacitive coupling, and therefore allowed (with no bias applied) the highest energy ions to be kept below the reported threshold of 16 eV,[23] especially at higher pressures. When the plasma was OFF, a narrow (full width at half maximum <2 eV) IED could be obtained due to the drastically lower electron temperature. The energy of the sharp IED could be controlled by varying the dc bias on the boundary electrode or the sample.[11,24] During the late afterglow, especially with addition of chlorine, the plasma potential was very low (close to 0 V) and the boundary electrode potential was approximately equal to the plasma potential. Hence, ion assisted etching, with a well-defined ion energy, should be confined to the afterglow, and then only during application of dc bias.

III. RESULTS AND DISCUSSION

A. Ion-assisted etching rates, thresholds, and yields

A 5×5 cm^2 piece of *p*-type Si was placed in the reactor, a pulsed Ar plasma (10 kHz, 20% duty cycle, 100–110 W average power) with a small addition (1%) of Cl_2 was ignited, and emission nearby the surface was collected by the periscope and analyzed with the monochromator. Optical emission spectra were similar to those reported by others during

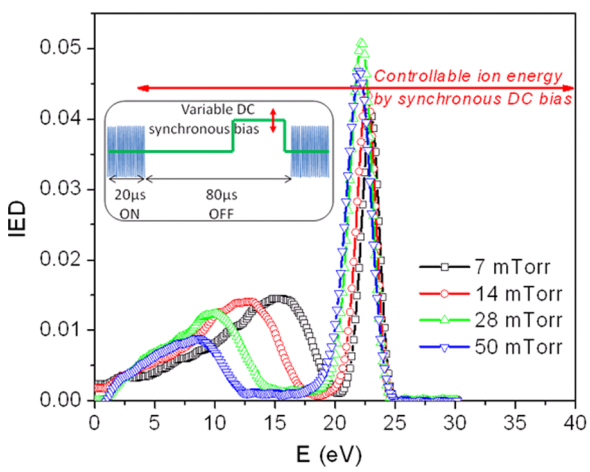

FIG. 4. (Color online) Ion energy distributions (IED) generated by applying a synchronous dc bias on a boundary electrode for a specified time window during the afterglow of a pulsed argon plasma. The broad lower energy peaks originate from the active glow; the sharp higher energy peaks are due to the dc bias in the afterglow. The IED can be controlled by the gas pressure to have no ions with energy higher than the etching threshold (16 eV). The energy of the nearly monoenergetic peak of the IED can be controlled by varying the dc bias. (Reproduced from Ref. 11.)

etching of Si in a chlorine plasma,[25–27] except for less emission from Cl and Cl_2 for the present Cl_2-dilute conditions. Si emission lines were identified between 2507 and 2882 Å. The strongest 2882 Å line was used to monitor Si removal by etching. The SiCl bands also appeared at 2807 Å and 2824 Å and behaved similarly to the Si emission as a function of plasma conditions. Other Si etching products that give rise to $SiCl_2$ and $SiCl_3$ emission bands around 3300 and 3850 Å, respectively, also showed behavior similar to the Si signal.

The Si emission at 2882 Å was recorded at several pressures as the synchronous dc bias on the boundary electrode, applied late in the afterglow ($t = 70$–$98\ \mu s$), was varied. The sample was cleaned by Ar sputtering before each run and a number of points were collected at random bias to minimize systematic errors. Relative Si emission intensities are plotted as a function of the square root of ion energy, E (= afterglow bias voltage), in Fig. 5. Absolute etching rates were measured by laser interferometry at 50 mTorr and three bias voltages (hollow triangle symbols). The relative Si emission intensities at 50 mTorr were normalized with a single constant to match these measurements. The agreement between relative emission intensities and etching rates shows that the emission measurements provide etching rates as a function of ion energy at 50 mTorr. It should be noted that Si emission is expected to be proportional to etching rate at any given pressure, but the comparisons between different pressures require corrections for the pressure-dependent effects of electron density and energy distributions on the Si optical emission intensity (not done here).

As shown in Fig. 5, etching rates at any pressure were constant until the ion energy reached 16 V, above which the etching rate increased nearly linearly versus $E^{1/2}$. The ion-assisted etching threshold was independent of pressure or the amount of chlorine addition (0.25–3 % Cl_2 in Ar). The ion-assisted etching threshold with chlorine was much smaller than the physical sputtering threshold (~45 eV) with Ar^+ ions, measured in the same manner using a pure argon

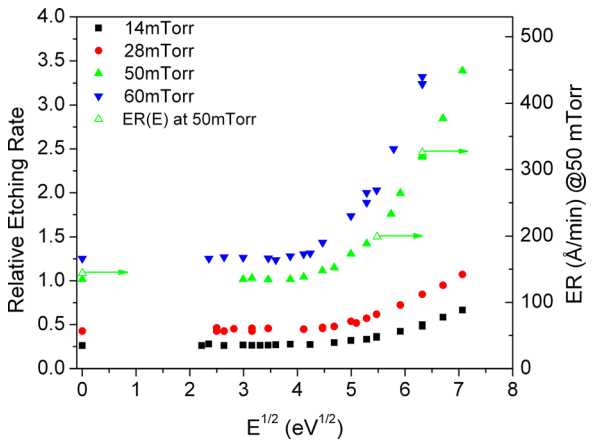

FIG. 5. (Color online) Relative etching rates (i.e., intensities of Si 2882 Å emission) at different pressures (left axis), and absolute etching rate at 50 mTorr (hollow triangles, right axis), as a function of $E^{1/2}$ (E = ion energy) in a 1%Cl_2/99%Ar plasma pulsed at 10 kHz with a duty cycle of 20%. The bias was applied 50 μs into the afterglow (i.e., at $t = 70\ \mu s$) until $t = 98\ \mu s$.

plasma. The ion-assisted etching threshold observed in this study is consistent with the 16 eV value reported by Chang *et al.*[23] using Ar^+ ions and Cl/Cl_2 in a beam system, conditions that most closely resemble those in the present study. When Cl^+ was substituted for Ar^+, Chang and Sawin[28] saw the threshold drop to 10 eV. Vitale *et al.*[29] found a 9 eV threshold, using a plasma beam system with a mixture of Cl_2^+ and Cl^+. Balooch *et al.*[30] reported the threshold for ion enhanced etching of Si by Cl_2 to be 25 eV for Cl_2^+ and 45 eV for Ar^+.

Above the threshold energy (16 eV), the relative etching rates in Fig. 5 show the usual linear dependence on the square root of ion energy,[31]

$$ER(E) = K(\sqrt{E} - \sqrt{E_{th}}) + C, \quad (1)$$

where E_{th} is the threshold ion energy, and K is a proportionality constant. The additional term, C, corresponds to Si etching by other mechanisms such as isotropic etching by Cl atoms or photo-assisted etching. The ratio of etching rate at 0 V bias to that above the threshold bias (e.g., 40 V) is higher at lower pressure, possibly due to the small fraction of ions above 16 eV at lower pressures during the active glow (broad peaks in Fig. 4). At higher pressures; however, this cannot explain the significant etching rate at bias voltages below the 16 eV threshold (Fig. 5). The origin of this sub-threshold etching is discussed below.

The ion-assisted etching yield (Y), the number of Si atoms removed per impinging ion (presumably mostly Ar^+), was calculated using the etching rate measured by laser interferometry and the measured ion fluxes (e.g., Fig. 2). The ion-assisted etching rate was computed by subtracting the etching rate at 0 eV from the total etching rate. For 30 and 40 eV ion energy, respectively, the etching yield was found to be 0.14 and 0.41. The neutral-to-ion flux ratio under these conditions was in the range 10–100. For comparison, the etching yield measured by Vitale *et al.*[29] was ~0.91 for 40 eV ions. The higher Y values may be due to the different positive ions [Cl_x^+, ($x = 1$ or 2) vs mostly Ar^+] and higher neutral-to-ion flux ratio (1000 s) in their measurements. Chang *et al.* measured a Y~0.4 for 35 eV Ar^+ ions for a neutral-to-ion flux ratio comparable to that in the present study.[23] Chang and Sawin[28] found that the etching yield can be enhanced by a factor of 2 by using Cl^+ instead of Ar^+ ions in their beam experiment.

B. Sub-threshold etching

In Fig. 5, it is noteworthy that there is a significant etching rate when the energy of ions during both the active glow and afterglow periods was kept below the 16 eV threshold for ion-assisted etching. It is widely reported that p-type Si does not etch in chlorine plasmas without ion bombardment.[32–34] This sub-threshold etching may make small contributions to the total etching rate in plasmas dominated by high energy ions. However, in plasma etching processes currently under development for precise and near-damage-free etching using low energy ions, the observed sub-threshold etching would be

substantial, and likely detrimental, since it will not allow etching with atomic layer accuracy, and it may also affect sidewall profile development.

Four potential mechanisms for sub-threshold etching are considered below: (1) spontaneous chemical etching by Cl atoms, (2) Ar metastable-assisted etching, (3) very low energy ($E<E_{th}$) ion-assisted etching, and (4) photo-assisted chemical etching. After systematic investigations, the sub-threshold etching of p-type Si with chlorine was attributed to photo-assisted chemical etching.

C. Spontaneous chemical etching by Cl atoms

Etching by Cl atoms in the absence of a plasma has been reported to be very slow near room temperature for *p*-type Si,[32–34] hence this does not appear to be the explanation for sub-threshold etching of *p*-type Si in the present study. Furthermore, etched profiles such as those in Fig. 6 show no undercutting of the Si below the SiO_2 mask. This sample was etched with an ion energy of 40 eV in the afterglow period. Under these conditions, the ion-assisted etching and sub-threshold etching rates are comparable. If spontaneous etching by Cl were the cause of sub-threshold etching, then the etched Si profile should exhibit an undercut just below the mask that would be about half of the etched depth. This is not the case. Consequently, spontaneous etching by Cl atoms can be ruled out.

D. Ar metastable-assisted etching

Ar metastables contain enough energy (11.55 and 11.72 eV for the $^3P_2$ and $^3P_0$ states, respectively) to cause desorption of $SiCl_x$ species and hence could stimulate etching. Such a process has never been reported, however, and seems very unlikely, given the nearly unit efficiency for quenching of rare gas metastables upon collisions with surfaces (e.g., 0.7 on smooth silica[35]), facilitated by the existence of nearby levels ($^3P_1$ and $^1P_1$) that radiate to the ground state. Nonetheless, to rule out Ar metastables, etching rates were measured as a function of bias voltage in a plasma containing only Cl_2. The plasma was generated in a *continuous wave* mode but the bias was applied during half of the 10 kHz cycle. (Fast electron attachment during the afterglow made it difficult to sustain a pulsed plasma using pure Cl_2 gas, particularly with the Faraday shield.) The results, presented in Fig. 7, look very similar to those in dilute Cl_2/Ar plasmas (Fig. 5). Ion-assisted etching starts at a bias voltage of about 12 V. This threshold is ~4 eV lower than that in Fig. 5 because of the higher plasma potential in the continuous wave plasma than the afterglow period of the pulsed Cl_2/Ar plasma, as well as the lower threshold for Cl^+ vs Ar^+.[28] Most importantly, there is a constant, nonzero etching rate below 12 eV, as with the dilute Cl_2/Ar pulsed plasma. This suggests a similar mechanism for sub-threshold etching in pure Cl_2 and Cl_2/Ar plasmas and rules out Ar metastables as the cause. In fact, the sub-threshold etching component in a pure Cl_2 plasma is even more substantial than in mostly Ar plasmas. In any case, the Ar metastable density should be depressed with addition of even small amounts of chlorine to an Ar plasma, due to the fast quenching of metastables by collisions with Cl_2.

E. Grid experiments that rule out very low energy ($E< E_{th}$) ion-assisted etching, and provide evidence for photo-assisted etching

When a positive ion approaches within a few Å of a surface, it is neutralized by an Auger process that creates a low energy electron.[36,37] It is possible that this electron (or hole left in the valence band), could cause a reaction in the chlorinated surface layer that would lead to etching. This mechanism would be possible even for ions with near-zero kinetic energy. To test this hypothesis, grids were placed above the substrate, as described above and depicted in Fig. 3(a), allowing etching to be carried out in the absence of any positive ion bombardment.

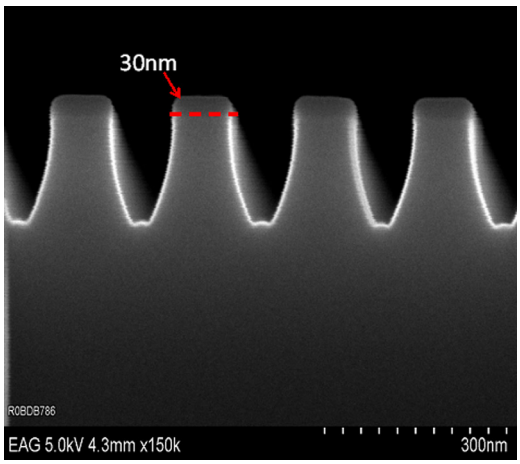

FIG. 6. (Color online) Cross sectional scanning electron micrograph (SEM) of a p-type Si sample, patterned with 100 nm lines and 100 nm spaces. The SiO_2 mask is 30 nm thick. The sample was etched in a pulsed 1% Cl_2/99% Ar plasma at 50 mTorr with a synchronous 40 V dc bias applied 50 μs into the afterglow (i.e., at $t = 70\ \mu$s) until $t = 98\ \mu$s.

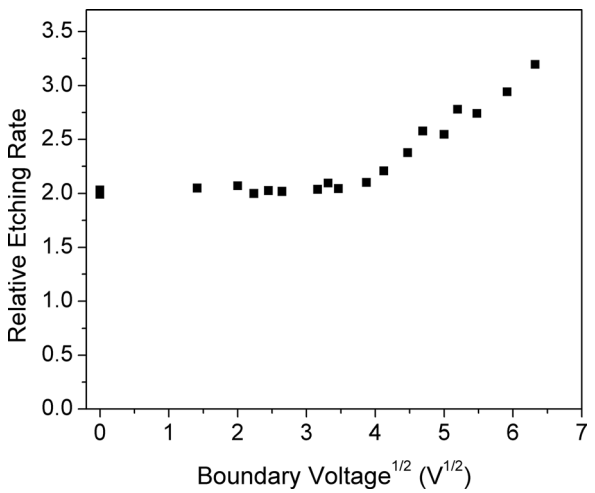

FIG. 7. Si emission intensity as a function of boundary electrode bias voltage in a pure Cl_2 plasma at 35 mTorr. The plasma was operated in a continuous-wave mode. Pulsed dc bias was applied with a frequency of 10 kHz and 50% duty cycle. Ion-assisted etching starts at around 12 V, which when added to the ~5 V plasma potential, results in a threshold energy of ~17 eV.

Figure 8 shows emission spectra in a continuous wave Ar/3% Cl_2 plasma at 300 W and 7 mTorr, at different biases on the sample (V_C). The spectra were collected using one sample. It took about one minute to collect one spectrum. Surface contamination was not an issue, as verified by repeated scans with the same bias. In all the cases, the atomic Si emission lines and two SiCl bands were observed in addition to Cl_2 emission bands. With 0 V bias, the ion energy was ~16 eV (near threshold) and Si and SiCl emissions were clearly observed. When the sample bias was changed to −30 V (~46 eV ion energy), the Si and SiCl emission intensities increased by about a factor of 3, as expected from the data in Fig. 5. However, when the sample was biased at +30 V, preventing all ions from reaching the Si surface, the Si and SiCl emission intensities were about the same as the 0 V bias case. This would seem to rule out any mechanism promoting sub-threshold etching that involves low energy ions.

The possible influence of charge exchange in distorting the results of the grid experiments must be considered. At 7 mTorr, ions in a continuous wave plasma enter the top grid [Fig. 3(a)] with a maximum energy of 20 eV, a peak energy of 16 eV and a tail with lower energies (see Fig. 4). In the nearly field-free 2 mm distance between the 2 grids, 10% (i.e., $100 \times [1-\exp(-2/18)]$, where the mean free path for charge exchange collisions is 18 mm) of these ions will suffer charge exchange and be converted into neutrals with the translational energy of the initial ions. If we assume that fast neutrals have identical etch yield as ions with the same energy, then from Fig. 4, roughly 1/3 of the ions at 7 mTorr enter the grid with energies above the 16 eV threshold, and hence only 3% (10% × 1/3) of the ions traversing the space between the grids are converted into fast neutrals that can induce etching.

Ions exiting the second grid are either accelerated or decelerated by negative or positive bias on the substrate. About 15% [i.e., $100 \times (1-\exp(-3/18))$] of the ions accelerated over the 3 mm distance to the substrate are converted into fast neutrals that could induce some etching. Since the ions in this case will mostly arrive at the sample with more energy that they entered the top grid, and the fast neutrals will have lower energies, the ion-assisted etching will be much enhanced (≈90% or higher) over fast neutral-assisted etching. When ions are decelerated, some additional neutrals are created, but these neutrals do not have sufficient energy to induce etching. Hence when positive bias is applied to repel all positive ions, the contribution by fast neutrals above the threshold for ion- (and fast neutral-) assisted etching is negligible.

In another experiment involving the grids, Si emission intensity at 2882 Å was recorded as a function of substrate bias that was repeatedly ramped from −30 to +30 V in each cycle lasting 20 s. At the same time, current to the sample was measured as a function of substrate bias voltage. A continuous wave 3% Cl_2/Ar plasma was operated at 7 mTorr. As shown in Fig. 9, an ion saturation current was measured between −30 and −12 V, with essentially no electrons reaching the sample at these voltages. As more positive voltage was applied, some current was collected from electrons that leaked through the grids. By +30 V substrate bias, all positive ions were repelled and only electrons reached the sample. (As mentioned above, even at the most positive substrate bias voltage, the plasma potential was not affected appreciably.) Si emission was a constant, nonzero value at bias voltages between +30 and ~+5 V and then began to increase as the bias voltage was made increasingly negative. Low energy ions (as well as low energy electrons) can be ruled out as the cause for sub-threshold etching, since at higher positive bias, no ions can reach the surface, yet a substantial etching rate persists. By process of elimination, it seems that photo-assisted etching is the most likely cause for the sub-threshold etching. Next, we present experiments

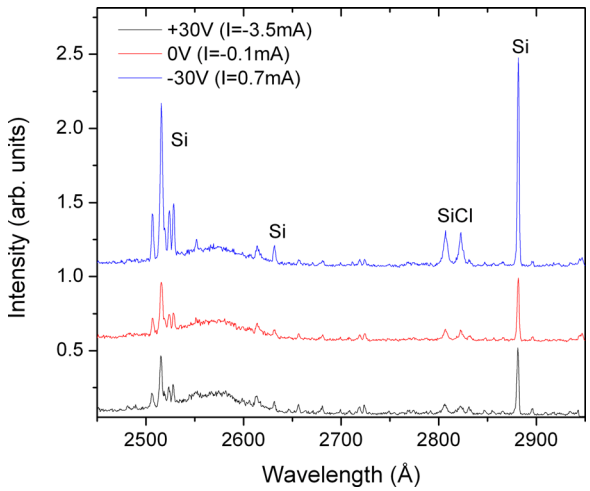

FIG. 8. (Color online) OES spectra taken during etching of p-type Si in a 7 mTorr continuous wave 3%Cl_2/97%Ar plasma with different bias voltages applied to the substrate. Application of a negative bias results in more intense Si emission, whereas positive bias and no bias show the same lower emission intensity. The current on the substrate measured for each case is given in parenthesis (top left corner).

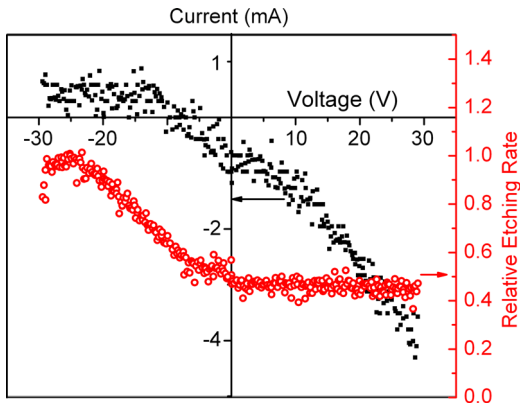

FIG. 9. (Color online) Current to the substrate and relative etching rate (i.e., intensity of Si 2882 Å emission) as a function of the bias voltage applied to the substrate. A continuous 3% Cl_2/Ar plasma was operated at 7 mTorr. The substrate bias was ramped from −30 to +30 V in 20 s. The ion saturation current is obtained between −30 and −12 V, with essentially no electrons reaching the substrate. With +30 V substrate bias, all positive ions are repelled and only electrons reach the substrate. Si emission is constant at bias voltages between +30 and +5 V, indicating no influence of low energy ions on etching of silicon.

indicating that photo-assisted is due mostly to short wavelength (<1700 Å) radiation.

F. Wavelength dependence for photo-assisted etching

In the experiment described in Fig. 3(b), most of the light from the plasma was blocked from reaching the surface beneath the opaque mask suspended above the sample, while light with wavelengths greater than 1700 Å was allowed to pass through the quartz plate and irradiate the surface. Presumably, the plasma and Cl atom densities in the 11 mm space between the quartz roof and the samples was similar over both samples. Etching was performed at 50 mTorr Ar, and 300 W continuous wave plasma, with 3% Cl_2 in Ar, and no applied bias. Samples of *p*-type Si were masked with Kapton tape and etched for 12 min. After etching, the tape was removed and the etched depth was measured in three locations with a stylus profilometer. The sample beneath the opaque mask was etched to a depth of 46 ± 6 nm, while that below the quartz window etched to a depth of 126 ± 11 nm. The enhanced etching in the region receiving a higher level of illumination can be attributed to photo-assisted etching as discussed above.

When the expected etching rate of the sample under the unblocked side of the quartz roof was compared to the etching rate actually measured, further insight into the photo-assisted etching was revealed. Starting with the etching rate at 50 mTorr with 0 V bias (144 Å/min) of Fig. 5, and correcting for the differences in power (100 W versus 300 W) and % Cl_2 (1% vs 3%), the etching rate should have been ~1300 Å/min. However, the observed etching rate under the unblocked side of the quartz window was 105 Å/min, only a small fraction (<10%) of the expected estimated value. This indicates that photo-assisted etching is dominated by short wavelength photons (< 1700 Å nm) that do not pass through quartz. Indeed, in Ar plasmas, strong vacuum ultraviolet (VUV) lines are emitted at 104.8 and 106.6 nm.[38,39] In this study, the VUV flux was not measured, but photon power densities of up to 52 mW/cm^2 have been reported in pure Ar ICPs, integrated over wavelengths between 50 and 250 nm (24–4.9 eV).[39]

Photo-enhanced etching is usually ascribed to a charge transfer process in which photoelectrons are captured by Cl (or F) and photo-generated holes aid in breaking Si–Si bonds.[3–5] A similar mechanism involving formation of Cl^- was proposed to explain the much faster etching rate by Cl atoms of heavily doped n^+-Si (~10^{20} cm^{-3}) compared with undoped or *p*-type Si.[3,32,34] Very high photo-sputtering yields (10–60 atoms per photon) have been reported for etching of Si by XeF_2 (Refs. 40, 41) and of GaAs by Cl_2 (Ref. 41) at such short wavelengths. Higher etching yields for VUV versus visible radiation could be due to hot carriers created by energies well above the bandgap energy, but it is difficult to explain yields much greater than unity.

The nearly equal contributions of photo-assisted and low-energy (~36 eV) ion-assisted etching of *p*-type Si in chlorine-containing plasmas is quite surprising, given that it has not been reported previously, but is likely to have unwanted effects on etched profiles. Quite often, profiles of Si etched in chlorine-containing plasmas exhibit a range of artifacts that until now have been attributed to mechanisms other than photo-assisted etching.[42,43] Most published studies of etched feature profile evolution in chlorine plasmas were carried out at higher ion energies, where ion-assisted etching is dominant, and a mechanism such as microtrench formation from glancing angle scattering of ions off feature sidewalls is likely to be correct. At low ion energies, however, photo-assisted etching is playing an additional role in profile development. For example, when photo-assisted etching dominates, microtrenches are observed at the bottoms of sidewalls of etched features (Fig. 10). The plasma-generated VUV photons from Ar at 104.8 and 106.6 nm are repeatedly absorbed by ground state Ar and re-emitted until they emerge for the periphery of the plasma. Those striking the Si substrate will be absorbed near the surface, with a 1/*e* absorption depth of about 8 nm,[44] generating electron hole pairs. The minority carrier (i.e., electrons) diffuse to the surface and enhance etching. However, at a glancing incidence angle, those photons can be reflected from sidewalls and enhance etching adjacent to the sidewalls. Therefore, the mechanism can be analogous to ion scattering, where photons are specularly reflected off sidewalls, enhancing illumination intensities at the base of the etched feature. Diffraction will also play a role in enhanced intensity at selected locations adjacent to etched features.

The profiles in Fig. 6 have sloped walls but no undercutting of the mask. Similar sloped wall with minimal undercutting was reported by Okano *et al.* for etching Si in the presence of Cl_2 with UV light incident on the surface.[3] The profiles were particularly sloped if the angle of incidence of the light was off-normal. In a plasma, profiles will exhibit a combination of near-vertical sidewalls from ion-induced etching and sloped sidewalls from the wide angular spread of incident light from the diffuse plasma glow. When the ion-assisted and photo-assisted rates are comparable, profiles such as those in Fig. 6 could be expected. It is also expected

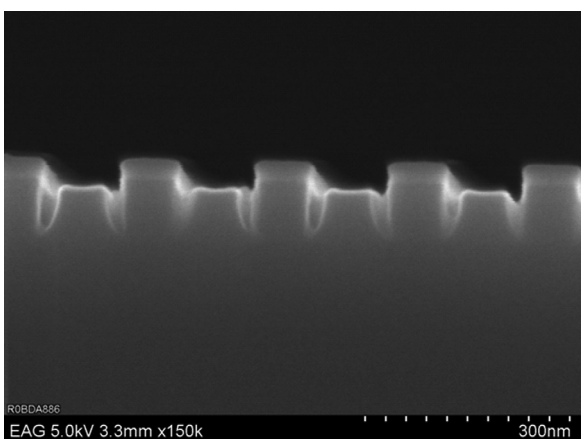

FIG. 10. Cross sectional SEM of a patterned p-type Si sample after 10-min etching in 1%Cl_2/99% Ar pulsed plasmas at 50 mTorr with no synchronous dc bias during afterglow. At this pressure, all ions have energy less than etching threshold (16 eV) but microtrenches are observed due to photo-assisted etching.

that the photo-assisted etching rate would become small inside trenches that are smaller than the wavelength of light emitted from the plasma. Photo-assisted etching is also detrimental for processes that require monolayer accuracy (e.g., atomic layer etching[45,46]). In order to achieve atomic layer control, etching must occur only when the surface is exposed to an energetic flux of ions with controlled energy. If spontaneous or photo-assisted etching occurs, the process is not self-limiting, compromising atomic layer resolution.

It is conceivable that the sub-threshold Si emission signal originates from silicon deposits on the chamber walls, rather than the silicon sample. It was verified that this is not the case by lowering the sample out of the plasma region (~1 ft below the nominal sample location). The Si emission signal was then measured to be only a few percent compared to the signal when the unbiased sample was in the plasma, while the SiCl signal completely disappeared. In addition, etching under sub-threshold ion energy was observed directly by IR laser interferometry (Fig. 5, hollow triangle at 0 eV) and SEM examination of a sample etched without bias (see Fig. 10).

IV. SUMMARY AND CONCLUSIONS

Si etching was investigated using a nearly monoenergetic ion energy distribution (IED) in a plasma containing a few % Cl_2 in Ar. A monoenergetic ion energy was obtained by applying a synchronous dc bias on a boundary electrode during a specified time window in the afterglow of a pulsed plasma sustained in a Faraday-shielded ICP reactor, allowing the ion energy dependence of Si etching to be directly measured in the plasma. A threshold energy of $E_{th} = 16$ eV was measured for ion-assisted etching, in agreement with published beam studies. Above threshold, the etching rate scaled with ion energy, E, as $\propto (E^{1/2} - E_{th}^{1/2})$, also in agreement with published accounts.

Surprisingly, considerable etching of *p*-type silicon was observed, independent of energy, even for ions with energies below the 16 eV threshold. Such "sub-threshold etching" of *p*-type Si *in a plasma* has not been reported previously. Etched features showed no mask undercut, confirming that there was no spontaneous etching of *p*-type Si by Cl atoms. Ar metastables could not be responsible either, since sub-threshold etching was also observed in pure chlorine plasmas. Furthermore, ions with sub-threshold energy were shown not to cause etching: when all ions were repelled from the sample surface, sub-threshold etching persisted. Finally, by using grids to prevent ions from reaching the sample, while allowing most of the plasma-generated light to irradiate the sample, it was shown conclusively that the sub-threshold etching was due to photo-assisted etching by chlorine. In particular, it was found that photo-assisted etching was dominated by light with wavelength less than 1700 Å.

For *p*-type and presumably undoped or lightly doped *n*-type Si, the photo-assisted etching rate is significant, compared to ion-assisted etching, for processes that require low ion energies (10s of eV) to achieve high selectivity and low damage, such as atomic layer etching. Under these conditions, photo-assisted etching likely plays an important role in the evolution of features with sloped sidewalls during Si etching in chlorine-containing plasmas.

ACKNOWLEDGMENTS

This work was supported by the Department of Energy, Office of Fusion Energy Science, Contract No. DE-SC0001939, the National Science Foundation Grant No. CBET 0903426, the Department of Energy Grant No. DE-SC0000881, and Varian Semiconductor Equipment Associates (VSEA). Many thanks to Ludovic Godet of Varian Semiconductor Equipment Associates, for SEMs and for providing patterned Si samples.

[1] J. W. Coburn and H. F. Winters, J. Appl. Phys. **50**, 3189 (1979).
[2] S.-B. Wang and A. E. Wendt, J. Vac. Sci. Technol. A **19**, 2425 (2001).
[3] H. Okano, Y. Horiike, and M. Sekine, Jpn. J. Appl. Phys. **24**, 68 (1985).
[4] N. Cabrera and N. F. Mott, Rep. Prog. Phys. **12**, 163 (1949).
[5] H. F. Winters, J. W. Coburn, and T. J. Chuang, J. Vac. Sci. Technol. B **1**, 469 (1983).
[6] F. A. Houle, Phys. Rev. B **39**, 10120 (1989).
[7] R. Kullmer and D. Bäuerle, Appl. Phys. A **43**, 227 (1987).
[8] P. Mogyorósi, K. Piglmayer, R. Kullmer, and D. Bäuerle, Appl. Phys. A **45**, 293 (1988).
[9] R. B. Jackman, H. Ebert, and J. S. Foord, Surf. Sci. **176**, 183 (1986).
[10] S. Samukawa, B. Jinnai, F. Oda, and Y. Morimoto, Jpn. J. Appl. Phys. **46**, L64 (2007).
[11] H. Shin, W. Zhu, L. Xu, V. M. Donnelly, and D. J. Economou, Plasma Sources Sci. Technol. **20**, 055001 (2011).
[12] M. R. Wertheimer, A. C. Fozza, and A. Holländer, Nucl. Instrum. Methods Phys. Res. B **151**, 65 (1999).
[13] D. Nest, D. B. Graves, S. Engelmann R. L. Bruce, F. Weilnboeck, G. S. Oehrlein, C. Andes, and E. A. Hudson, Appl. Phys. Lett. **92**, 153113 (2008).
[14] E. Pargon, M. Martin, K. Menguelti, L. Azarnouche, J. Foucher, and O. Joubert, Appl. Phys. Lett. **94**, 10311 (2009).
[15] J. Lee and D. B. Graves, J. Phys. D **44**, 325203 (2011).
[16] I. Tanarro and V. J. Herrero, Plasma Sources Sci. Technol. **18**, 034007 (2009).
[17] F. B. M. Copeland and D. S. F. Crothers, At. Data Nucl. Data Tables **65**, 273 (1997).
[18] S. H. Pullins, R. A. Dressler, R. Torrents, and D. Gerlich, Z. Phys. **214**, 1279 (2000).
[19] V. M. Donnelly and J. A. McCaulley, J. Vac. Sci. Technol. A **8**, 84 (1990).
[20] V. M. Donnelly, D. L. Flamm, C. W. Tu, and D. E. Ibbotson, J. Electrochem. Soc. **129**, 2533 (1982).
[21] V. M. Donnelly, J. Vac. Sci. Technol. A **10**, 1060 (1992).
[22] J. A. McCaulley, V. M. Donnelly, M. Vernon, and I. Taha, Phys. Rev. B **49**, 7408 (1994).
[23] J. P. Chang, J. C. Arnold, G. C. H. Zau, H.-S. Shin, and H. H. Sawin, J. Vac. Sci. Technol. A **15**, 1853 (1997).
[24] H. Shin, W. Zhu, V. M. Donnelly, and D. J. Economou, "Ion energy distributions, electron temperatures and electron densities in Ar, Kr and Xe pulsed discharges," J. Vac. Sci. Technol. A (submitted).
[25] J. Y. Choe, I. P. Herman, and V. M. Donnelly, J. Vac. Sci. Technol. A **15**, 3024 (1997).
[26] V. M. Donnelly, M. V. Malyshev, M. Schabel, A. Kornblit, W. Tai, I. P. Herman, and N. C. M. Fuller, Plasma Sources Sci. Technol. **11**, A26 (2002).
[27] V. M. Donnelly, J. Vac. Sci. Technol. A **14**, 1076 (1996).
[28] J. P. Chang and H. H. Sawin, J. Vac. Sci. Technol. A **15**, 610 (1997).
[29] S. A. Vitale, H. Chae, and H. H. Sawin, J. Vac. Sci. Technol. A **19**, 2197 (2001).
[30] M. Balooch, M. Moalem, Wei-E. Wang, and A. V. Hamza, J. Vac. Sci. Technol. A **14**, 229 (1996).
[31] C. Steinbrüchel, Appl. Phys. Lett. **55**, 1960 (1989).
[32] E. A. Ogryzlo, D. E. Ibbotson, D. L. Flamm, and J. A. Mucha, J. Appl. Phys. **67**, 3115 (1990).
[33] C. J. Mogab and H. J. Levinstein, J. Vac. Sci. Technol. **17**, 721 (1980).
[34] D. L. Flamm, Pure Appl. Chem. **62**, 1709 (1990).

[35]P. Macho and N. Sadeghi, Plasma Sources Sci. Technol **13**, 303 (2004).
[36]H. D. Hagstrum and G. E. Becker, Phys. Rev. B **8**, 1580 (1973).
[37]H. D. Hagstrum, Phys. Rev. **96**, 325 (1954).
[38]J. R. Woodworth, M. G. Blain, R. L. Jarecki, T. W. Hamilton, and B. P. Aragon, J. Vac. Sci. Technol. A **7**, 3209 (1999).
[39]J. R. Woodworth, M. E. Riely, V. A. Amatucci, T. W. Hamilton, and B. P. Aragon, J. Vac. Sci. Technol. A **19**, 3209 (2001).
[40]U. Streller, B. Li, A. Krabbe, H.P. Krause, I. Twesten, and N. Schwentner, J. Electron Spectrosc. Related Phenom. **80**, 49 (1996).
[41]U. Streller, B. Li, A. Krabbe, and N. Schwentner, Appl. Surf. Sci. **96–98**, 488 (1996).
[42]M. A. Vyvoda, M. Li, D. B. Graves, H. Lee, M. V. Malyshev, F. P. Klemens, J. T. C. Lee, and V. M. Donnelly, J. Vac. Sci. Technol. B **18**, 820 (2000).
[43]A. P. Mahorowala, H. H. Sawin, R. Jones, and A. H. Labun, J. Vac. Sci. Technol. B **20**, 1055 (2002).
[44]D. F. Edwards, *Handbook of Optical Constants of Solids*, edited by E. D. Palik (Academic Press, Orlando, 1985), pp. 547–569.
[45]S. D. Athavale and D. J. Economou, J. Vac. Sci. Technol. A **13**, 966 (1995).
[46]S. D. Athavale and D. J. Economou, J. Vac. Sci. Technol. B **14**, 3702 (1996).